TOPOGRAPHIC DESCRIPTORS AND THERMAL INVERSIONS AMID THE PLATEAUS AND MOUNTAINS OF THE JURA (FRANCE)

Daniel JOLY [1] et Yves RICHARD [2]

[1] **Laboratoire ThéMA, CNRS and Université Bourgogne Franche-Comté**
Besançon, France
daniel.joly@univ-fcomte.fr

[2] **Centre de Recherches de Climatologie / Biogéosciences, CNRS and Université Bourgogne Franche-Comté**
Dijon, France
Yves.richard@u-bourgogne.fr

Abstract

Sixteen temperature measurement sites under forest cover are distributed across the plateaus and mountains of the Jura (France). They are composed of pairs of stations located, one at the bottom of a topographic trough, the other at least 50 m higher in altitude. Three descriptors (station elevation, altitudinal difference (amplitude) between the two stations of each site, and topographical context) are used to explain how the frequency, intensity, and duration of inversions are spatially structured. Depending on whether one considers: 1) tn (minimum temperature) or tx (maximum temperature), 2) frequency or intensity, the sign of the correlation values changes. This reflects the fact that not all inversions can be explained in the same way. Elevation moderately explains the three characters of the inversions. Amplitude mainly explains their frequency (R = -0.83 for daily minima [tn]) and their intensity (R = 0.62 for daily maxima [tx]). The magnitude of the topographic depressions where the low stations are located mainly explains the tn inversions while the magnitude of the eminences where the high stations are located mainly explains the tx inversions. Finally, a multiple regression where the explanatory variables correspond to the topographic descriptors makes it possible to model the three inversion indicators.

Keywords: temperature under forest cover, elevation, topography, inversion, Jura.

Résumé

Descripteurs topographiques et inversions thermiques sur les plateaux et montagnes du Jura français

Seize sites de mesure de la température sous couvert forestier sont dispersés sur les plateaux et la montagne du Jura, en France. Ils sont composés de deux stations situées, l'une au fond d'un creux topographique, l'autre au moins 50 m plus haut en altitude. Trois descripteurs (altitude des stations, écart altitudinal (l'amplitude) entre les deux stations de chaque site, contexte topographique) sont mis à contribution pour expliquer comment se structurent spatialement la fréquence, l'intensité et la durée des inversions. Selon que l'on considère 1) le moment où se produisent les inversions (tn, température minimale ou tx, température maximale), 2) la fréquence ou l'intensité, le signe des valeurs de corrélation change. Cela reflète le fait que toutes les inversions ne peuvent pas être expliquées de manière uniforme. L'altitude explique modérément les trois caractères des inversions. L'amplitude explique surtout leur fréquence (R=-0.83 lors des minimums journaliers[tn]) et l'intensité des inversions sur les maximums journaliers [tx] (R=0.62). L'ampleur de la dépression topographique où est situé le capteur-bas explique surtout les inversions qui se produisent sur les tn tandis que l'ampleur de l'éminence où est située le capteur-haut explique surtout les inversions observées sur les tx. Enfin, une régression multiple où les variables explicatives correspondent au descripteurs topographiques permet de modéliser les trois indicateurs des inversions.

Mots-clés : température sous couvert forestier, altitude, topographie, inversion, Jura.

Introduction

The number of studies of temperature inversions has increased in recent decades in relation to pollution phenomena (El Melki, 2007; Chemel *et al*., 2016; Largeron and Staquet, 2016; Czarnecka and Nidzgorska-Lencewicz, 2017). The origin of temperature inversions is first and foremost related to atmospheric conditions. At temperate latitudes, the most frequent inversions

are radiation inversions due to the radiative deficit at the surface that often occurs under anticyclonic conditions (Conangla *et al*., 2018). These radiative inversions develop preferentially under clear, windless skies at night (Barry, 2008; Joly and Richard, 2019). Inversions are often destroyed in the early morning hours by convective turbulence (Anquetin *et al*., 1998). However, if weather conditions allow, they may last several days (Vitasse, 2017). In such instances, disturbed weather, accompanied by humid air advections and cloudiness, ends the inversion sequence (Williams and Thorp, 2015). There is another type of inversion that is quite frequent in temperate latitudes (Barry, 2008; Mirocha and Branko, 2010; Dupont *et al*., 2016; Young, 2016; Yu *et al.*, 2017). These are the subsidence inversions that occur under hot, high pressure conditions at high altitudes by adiabatic air compression. They affect large areas and are responsible for the cloud seas that cover plains and valleys while only the summits remain clear.

Inversion phenomena are initiated or reinforced by local topography (Anquetin *et al*., 1998; Fallot, 2012). Because it is denser than warmer air, cold air migrates down slopes and accumulates at the bottom of depressions (Helmis and Papadopoulos, 1996; Papadopoulos and Helmis, 1999; Mahrt *et al*., 2010; Fernando *et al*., 2013; Burns and Chemel, 2015). The boundary layer that develops in such contexts is totally decoupled from the overlying synoptic flow (Lundquist *et al*., 2008; Daly *et al*., 2009; Dorninger et *al*., 2011; Largeron and Staquet, 2016).

To be as rigorous as possible, inversions should be studied from equivalent potential temperatures to take into account the effects of elevation, saturation, and changes in water status. Since a majority of weather stations do not measure pressure or humidity, most of the work is based only on temperature, as is the present study. Within the framework of the "Zone Atelier de l'Arc Jurassien" (https://zaaj.univ-fcomte.fr/), a network of 29 sensors was installed under forest cover (UFC) in the Jura region (France) in spring 2011 (Joly, 2014). This network was expanded at the end of 2014 by 20 other sensors to extend the observation area to the east and northeast. This larger network revealed that the same regressors explain the spatial variation of temperature in open sites and UFC (Joly and Gillet, 2017). This same network was the basis for further research to study the frequency, intensity, and duration of inversions during the three years of observation (Joly and Richard, 2019). The current contribution continues the previous study. Its challenges are to determine the rules that allow a better understanding of the role of topography in the setting and development of inversions in a medium-sized mountain region where pollution by wood heating is ubiquitous.

Accordingly, the objective of this study is to analyze the influence of topography on the characteristics of inversions (frequency, intensity, and duration) observed across the plateaus and mountains of the Jura (eastern central France). For that, we use daily minimum (tn) and maximum (tx) temperature records from 16 sites composed of two stations, one at the bottom of the depression (low station) and the other at the top of the slope (high station). The influence of topography will be examined through five descriptors: the elevations of the low and high stations, the altitudinal amplitude between the stations composing each pair, the depth of the depression within which the low station is located and the magnitude of the hump on which the high station is located. The depth of the depression and the magnitude of the hump are defined in Joly *et al.* (2012). Finally, particular attention will be paid to statistical modeling by multiple regression to estimate the three inversion characters.

1. Data and method

The study area (figure 1), in the French part of the Jura massif, is characterized by a mountain climate with a continental tendency (Joly *et al*., 2010). Under the Köppen climate classification

system, the study area is of the Cfb type (temperate oceanic climate C = temperate, f = no dry season, b = warm summer) up to about 1000 m a.s.l. and at higher elevations it is of the Cfc type (c = cold summer). It is bordered by the Doubs valley to the north and by the Jura ridges to the east and south. To the west, it does not extend beyond the first plateau of the Jura. All three topographical groups of the Jura are represented: the low land (200–250 m) to the north, the two plateaus (300–600 m) in an intermediate location, and the high range up to 1000 m.

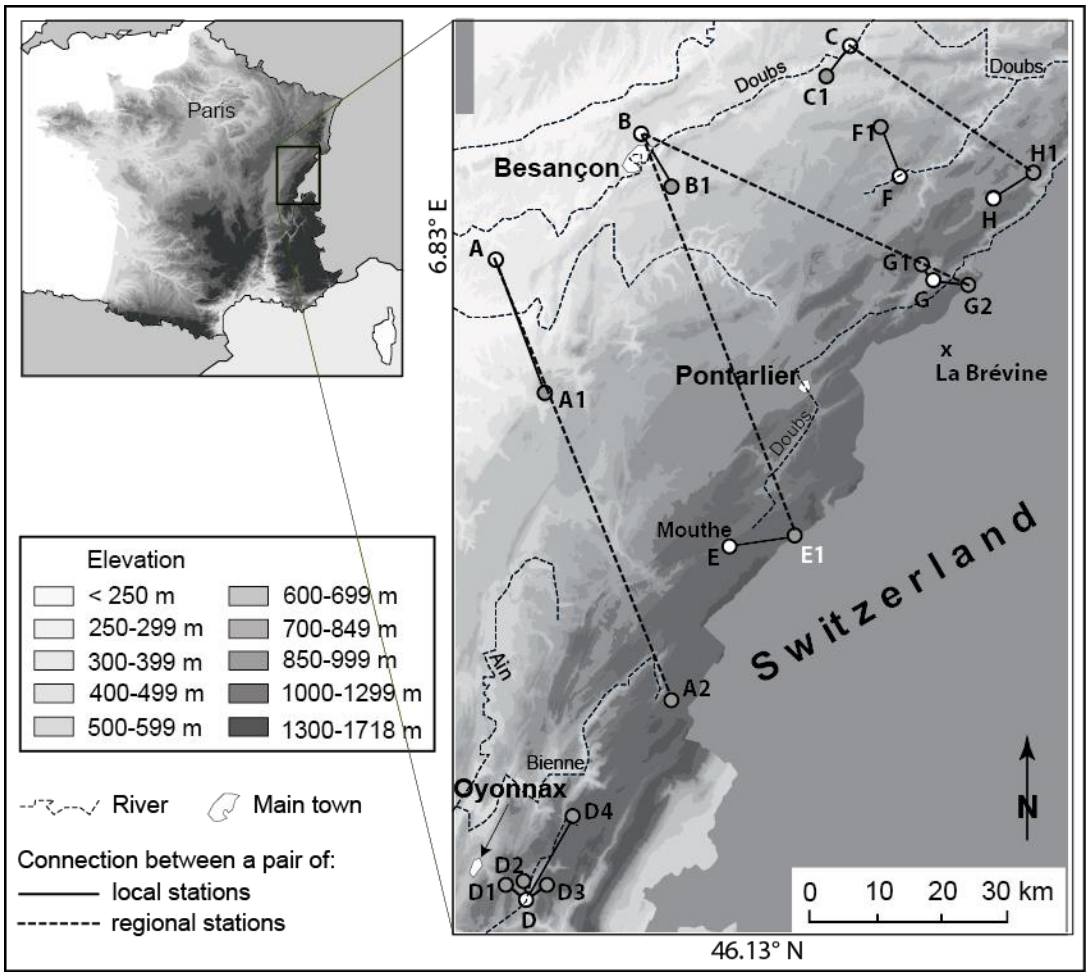

Figure 1. Study area and location of stations. Stations in the lower position are marked with a letter without numbers. *Aire d'étude et localisation des capteurs. Les stations situées en position basse sont repérées par une lettre sans chiffre.*

1.1. Data

It should be noted first and foremost that, in this paper, the term "sensor" refers to the device used to measure temperature and "station" refers to the measurement points managed either by the official institutions accredited by the WMO or the elements of our own network under forest cover that we have set up in the Jura. Since two low stations can be connected to several high stations, the analyses will focus on 16 pairs of stations that will be referred to as "sites" in the paper.

A network of 48 temperature stations under forest cover was installed at the end of 2014 by one of the authors of this article in connection with the Parc Regional Naturel du Haut-Jura. The stations were first positioned so that they could be paired with one of the 25 weather stations in the Météo-France (MF) network located in a nearby open site. The remaining 23 are used to

sample specific sites omitted by MF stations, such as steep slopes or deep valley bottoms. For details of the localization of MF stations see Figure 1 in Joly and Richard (2019).

The inversion study is based on a comparison of temperatures collected at all the available pairs of stations, one at the bottom of the depression, the other higher up on a ridge or on an upper slope. The low stations refer to the eight stations located at the bottom of the topographic depression (valleys, synclines). These are paired with one or more stations located at least 50 m higher. The pairings are also based on a distance criterion. A first type of matching is done with the nearest station(s) within 20 km to analyze local inversions (figure 1). The 20 km range was chosen to ensure the two stations belong to the same topographic unit. The average distance and altitudinal amplitude between the stations composing each local pair are 8.5 km and 250 m respectively. The elevations of the lower stations range from 265 m (A) to 1047 m (E1) (Table 1). The second type of matching is done with the station(s) located more than 40 km apart, which corresponds to the minimum distance between the crests of the Jura and the bordering plain. These regional pairs are based on the three low-stations located around the Jura arc, at less than 330 m elevation (A, B, and C in figure 1), and on the four high stations that line the ridges of the Jura between 981 and 1235 m. The average distance and altitudinal amplitude between the stations of each regional pair is 58 km and 830 m. The elevation of the high stations ranges from 981 m (H1) to 1235 m (G2).

Local stations	**Elevation low station**	**Elevation high station**	**Amplitude**	**Topography low station**	**Topography high station**
A-A1	265	475	210	WV	P
B-B1	326	431	105	WV	P
C-C1	320	437	117	WV	P
D-D1	542	929	387	NV	S
D-D2	542	727	185	NV	US
D-D3	542	969	427	NV	US
D-D4	542	1103	561	NV	P
E-E1	1047	1228	181	WV	US
F-F1	536	710	174	NV	P
G-G1	801	1005	204	WV	US
G-G2	801	1235	434	WV	S
H-H1	883	981	98	WV	S
Regional stations	**Elevation low station**	**Elevation high station**	**Amplitude**	**Topography low station**	**Topography high station**
A-A2	265	1117	852	WV	P
B-E1	326	1228	902	WV	US
B-G2	326	1235	909	WV	S
C-H1	320	981	661	WV	S

Table 1. Characters of station pairs; WV = wide valley, NV = narrow valley, P = plateau, S = summit, US = upper slope. *Caractères des paires de stations ; WV = vallée large, NV = vallée étroite, P = plateau, S = sommet, US = haut de versant.*

Temperature under forest canopy (UFC) was measured by 21 sensors every 6 minutes using HOBO PRO V2 type sensors fitted in protective cases (Joly, 2015) fastened to the north side of trees 2 m above the ground (Kollas *et al.*, 2013). The recordings run from 1 January 2015 to 31 December 2017 with 2.6% of data missing. The daily minimum and maximum readings are extracted from the database. Since the highest altitudinal amplitude of the local station pairs is 551 m and the lowest amplitude of the regional station pairs is 661 m, there is continuity between the two types of stations (figure 2).

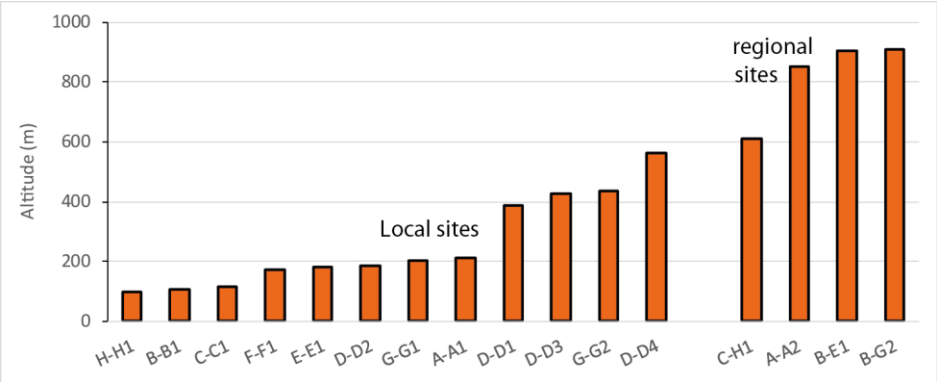

Figure 2. Altitudinal amplitude of local and regional sites running from 1 January 2015 to 31 December 2017.
Amplitude altitudinale des sites locaux et régionaux ayant fonctionné du 1 janvier 2015 au 31 décembre 2017.

1.2. Topographic descriptors

Several descriptors were derived from the 50 m resolution IGN (Institut Géographique National) digital terrain model (DTM) to assess the influence of topographical factors on inversions. In accordance with the results of Joly *et al*. (2012), five topographic descriptors (in square brackets) were chosen:

- (1) Elevation of the low [elev-low] and (2) high stations [elev-high].
- (3) Altitudinal amplitude [ampl], *i.e.* the difference in elevation (m) between the high station and the low station.
- (4) Depth of the valley [valley] where the low stations are located and (5) magnitude of positive relief (ridge, hills [hump]) where the high stations are located. Hump and valley are used to evaluate the height or depth of positive or negative relief relative to a topographic reference point (Joly *et al.*, 2012).

Other variables such as slope orientation and the density of direct solar radiation received at the high station were not used. Preliminary tests showed they had no significant influence on the frequency of the inversions measured.

Figure 3 shows the main indicators of the statistical distribution of the five topographic descriptors. Three points are worth mentioning. First, the mean is quite close to the median except for amplitude for which there is a 100 m difference. Second, the narrow distributions of valley and hump at the bottom of the elevation scale contrast with the distributions of the other three much broader descriptors. This is explained by the fact that valley and hump measure the vertical extension of topographic shapes while the other three descriptors are related to elevations of points scattered over the territory or to a measure of the relative distance between two points (amplitude). It should be noted that the vertical extension of the valleys is greater than that of humps, reflecting the marked depth of the valleys that are cut into the plateaus compared to the prominence of humps. The third aspect is the close proximity of the maximum and Q3 to the elevation of the high stations (1235 and 1227 m). This is due to the use of the four stations along the Jura ridges (A2, E1, G2, and H1) to compose three local and three regional sites.

1.3. Method

As in Joly and Richard (2018), a simple temperature difference is calculated. This difference is neither weighted nor normalized by the altitudinal amplitude. It is calculated separately for daily tn and tx and between each pair of stations by subtracting the temperature value recorded

at the low station from the values at the high station. A negative result indicates a thermal inversion, with the temperature being lower at the bottom than at the top.

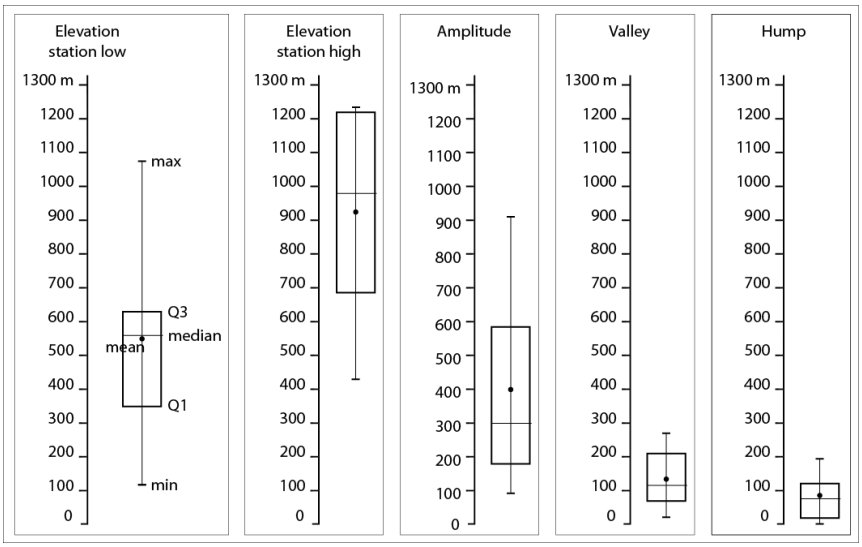

Figure 3. Box plot of the five topographic descriptors (altitude of the low and high stations of each pair, vertical amplitude between the two stations, depth of the valley, and extent of the prominence where the low and high stations are respectively located). *Box plot des cinq descripteurs topographiques (altitude des stations basses et hautes de chaque paire, amplitude verticale entre les deux stations, profondeur de la vallée et ampleur de la proéminence où sont respectivement localisées la station basse et la station haute).*

Three indicators are calculated: the average frequency, intensity, and duration of inversions for each of the 16 sites. Frequency is the number of inversions occurring during the three years of observation. Intensity is the temperature difference between the low station and the high station. Duration is minimal when the ephemeral inversion of late night and early morning disappears during the day. If the inversion continues into the afternoon or lasts even longer, it is referred to as an n-day sequence.

It should be noted that the values we will be working on are rough observed temperatures. It would have been possible to correct the temperatures to take into account the differences in altitudinal amplitude between the high and low stations at each site. This was not done for two reasons. The first is that this article follows a previous contribution (Joly and Richard, 2019) whose construction principles we wanted to maintain. The second is that this article is descriptive. It aims to reflect the sensory experience of any walker who feels the cold at the bottom of the troughs and the warm air a few tens of meters higher. This choice also makes it possible to explain the role of topography in the emergence of inversions that accounts for, at least partially, the differential distribution of snow (Pomeroy and Brun, 2001; Mernild and Liston, 2010).

The Bravais-Pearson correlation coefficient (R) is used to measure the dependence of the inversion characteristics on topographic factors. With a small sample, the risk of a result being random is high. This risk will be assessed by the p-value associated with each R.

3. Results

Very significant differences appear between sites (figure 4). The lowest inversion frequencies are 2.7% (site B-E1) and 3.5% (site A-A2) for tx and tn. They both concern regional sites. The highest values are for the local H-H1 (tn) and F-F1 (tx) sites and are 73.4% and 57.2% for tn and tx respectively. The minimum and maximum intensities are 0.6°C (tx, local site B-

B1) and 3.7°C (tn, local site G-G2) respectively. The average durations range from 1.3 days (local site B-B1) to 3.7 days (local site F-F1).

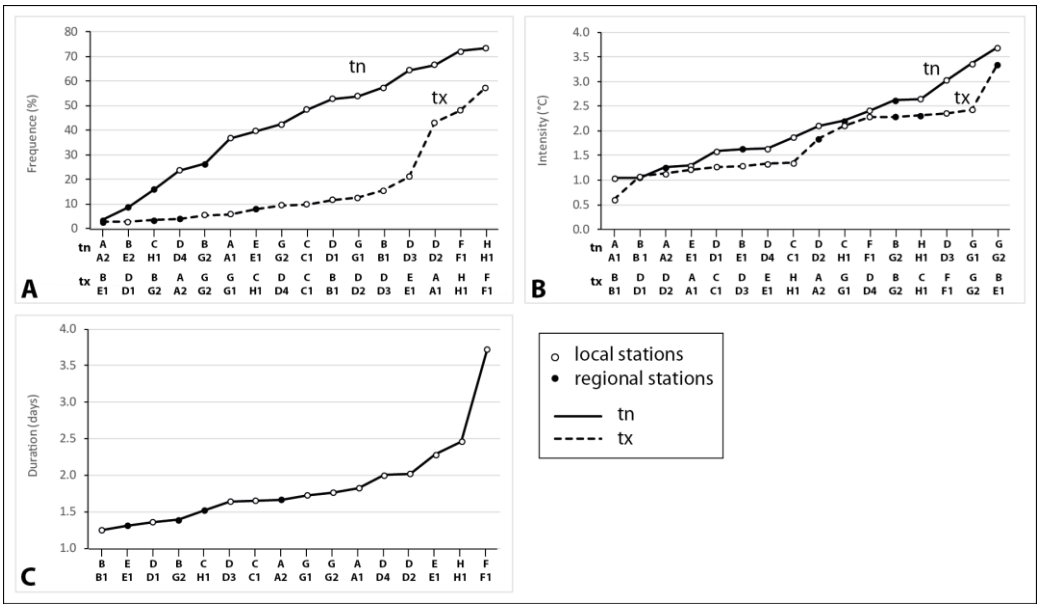

Figure 4. Mean (A) frequency, (B) intensity, and (C) duration of inversions for the 16 sites arranged in ascending order. Frequency and intensity differ with tn and tx, but not so duration. *Fréquence (A), intensité (B) et durée (C) moyennes des inversions (16 sites) rangées par ordre croissant. Il y a une différenciation concernant la fréquence et l'intensité selon les tn et les tx, mais pas pour la durée.*

The rather significant differences that appear between sites are probably explained by topographical factors. Four of them, easily quantifiable by topographic descriptors (elevation, altitudinal amplitude between the two loggers that make up each site, hump amplitude, and valley depth), are used to measure their influence on the frequency, intensity, and duration of inversions.

3.1. Influence of elevation

The correlation between the elevation of the high stations and the frequency of inversions is negative (Table 2, column 2). This means that the higher the elevation of the high station, the lower the frequency of inversions.

	low stations (1)	high stations (2)	Amplitude (3)	Valley (4)	Hump (5)
Frequency-tn	0.45*	-0.51**	-0.83***	0.42*	-0.15
Frequency-tx	0.21	-0.44*	-0.60**	-0.18	-0.40*
Intensity-tn	0.43*	0.30	-0.03	0.41*	0.67***
Intensity-tx	-0.07	0.57**	0.62***	-0.04	0.19
Duration	0.40*	-0.17	-0.50*	0.13	-0.36

Table 2: Correlation coefficient between frequency, intensity, and duration of inversions (tn and tx), and 1) elevation of low stations, 2) high stations, 3) altitudinal amplitude between the two stations of each site and according to the topographical context: 4) valley for low stations and 5) hump for high stations. R significant at the 10% (*), 5% (**), and 1% (***) levels. *Coefficient de corrélation entre les trois caractères (fréquence, intensité, durée) des inversions (tn et tx) et 1) altitude des stations basses, 2) altitude des stations hautes), 3) l'amplitude altitudinale entre les deux stations qui composent chaque site et selon le contexte topographique : 4) profondeur des vallées pour les stations-basses et 5) ampleur de l'émergence des reliefs pour les stations-hautes. R significatif au seuil de 10% (*), 5% (**) et 1% (***).*

Elevation has a positive influence on the intensity of inversions during tx (R=0.57), but no influence on the duration of inversions. On the contrary, the influence of elevation of the low stations on the frequency characteristics is positive (Table 2, column 1). The best scores concern the frequency and intensity of inversions during tn (R = 0.45 and 0.43) and the duration of inversions. Inversions are more frequent, more intense, and longer lasting when the low station is located at a high elevation, in the mountains, than when it is located on the plain or on the first plateau. These results seem to indicate that the upper valleys are the most suitable for inversions. This point is discussed further below.

3.2. Influence of the altitudinal amplitude

The altitudinal amplitude strongly influences the frequency of inversions (Table 2, column 3). This relationship is higher for the frequency of inversions-tn (R = -0.83) than for the frequency of inversions-tx (-0.60). In both cases it is negative: inversions are all the more frequent when the elevation difference between the low station and the high station is small.

A positive relationship is found for the altitudinal amplitude and intensity of inversions at tx (R = 0.62). This may be perceived as evidence of bias related to the fact that the calculated inversions are not normalized by the altitude amplitudes. Nevertheless, for tn, R is close to zero and reflects the statistical independence of altitudinal amplitude and intensity of inversions. The relationship between the altitudinal amplitude and the duration of the inversions is again negative (R = -0.50): the longer the inversion sequences, the smaller the elevation difference between the station pairs. This counterintuitive relationship will be discussed later.

3.3. Influence of hump amplitude and valley depth

Here again, the topographical context of the low station (depth of the valley where it is located) differs from that of the high station (magnitude of the hump eminence) (Table 2, columns 4 and 5). The influence of topographic landforms on inversion characteristics reveals similar arrangements to those described above. The frequency of inversions during tn is explained more by the depth of the valleys (valley, R = 0.42) and during tx by the prominence of the landforms (hump, R = -0.40). On the other hand, the intensity of inversions, for tn, is more strongly dependent on humps than on valleys. The intensity and duration of inversions during tx are more or less independent of the topographic context.

4. Calculation, by multiple regression, of the frequency, intensity and duration of inversions

Contrasting relationships have been highlighted: correlation coefficients are sometimes high (0.87), but often moderate (out of a total of 25, 14 are equal to or greater than 0.4). These results encourage us to estimate the frequency, intensity, and duration by multiple regression. The five descriptors explained are elevation of the low and high stations, altitudinal amplitude, valley (low station), and hump (high station).

As an example and in order not to overload the text, only one overview will be proposed: that relating to the frequency of inversions during tn. The progressive aggregation of an increasing number of regressors improves the quality of the regression model (Table 3). Even if the contribution of elev-low and hump is low, all explanatory variables contribute to the good final quality of the model.

The final equation is:

Frq_TN = 53.9 + (0.06*ampl) + (0.1*elev-low) - (0.1*elev-high) + (0.05*valley) + (0.6*hump)

	1	1+2	1+2+3	1+2+3+4	1+2+3+4+5
R^2	0.67	0.69	0.74	0.78	0.81
RMSE	49	47	44	40	38

Table 3: R^2 and RMSE obtained from five models aggregating, step by step, an increasing number of regressors; 1=ampl, 2=elev-low, 3=elev-high; 4=valley, 5=hump. *R^2 et RMSE obtenus de 5 modèles agrégeant, étape par étape, un nombre croissant de régresseurs ; 1=différence d'altitude entre les deux stations composant chaque site, 2=altitude de la station-bas, 3= altitude de la station-haut ; 4=profondeur de la vallée où est localisée la station-bas, 5=ampleur de la crête où est localisée la station-haut*

The result is very convincing since R^2 and RMSE are 0.81 and 9.8% respectively, while the regression, according to the Fisher test, is significant at the 2‰ level (Table 4). The cloud of the 16 estimated points is is tightly grouped along the regression line (figure 5).

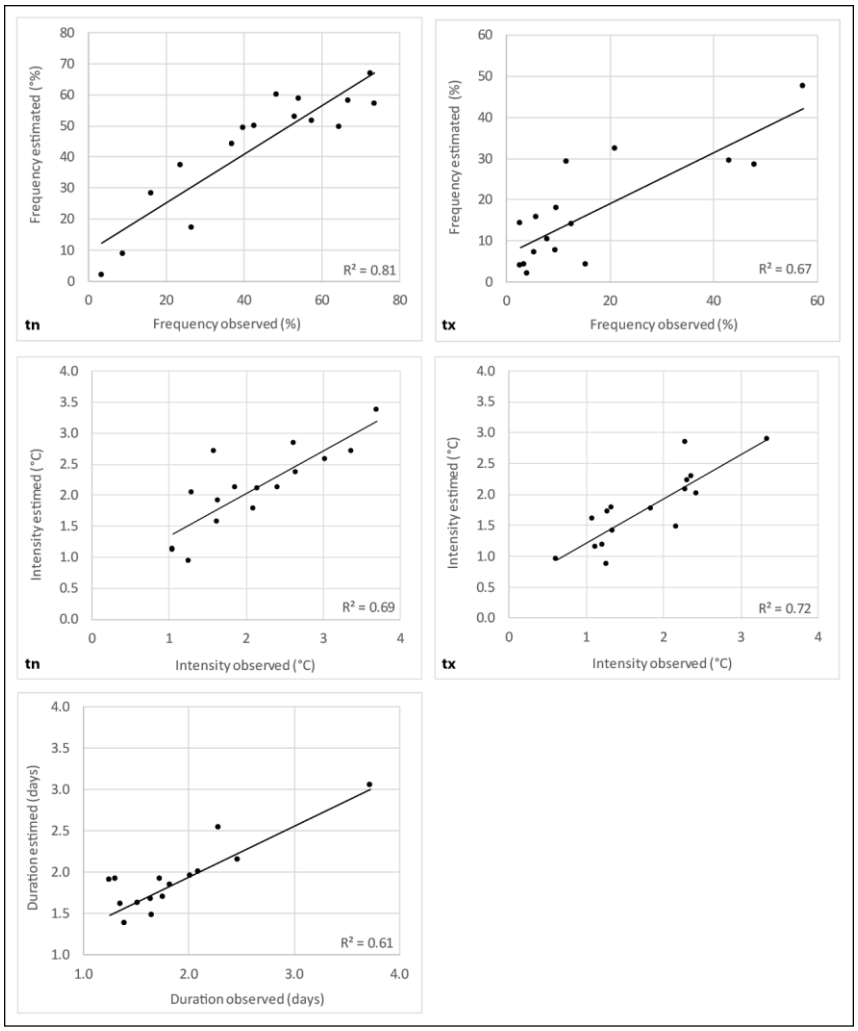

Figure 5. Scatterplots: observed values versus estimated values for the frequency (tn + tx), intensity (tn + tx), and duration of inversions. Estimates are made by multiple regression where the dependent variable is in turn the frequency, intensity, and duration of inversions and the explanatory variables are the five topographic variables described in Section 3 (altitude of low stations, altitude of high stations, altitudinal amplitude between the two stations that compose each site and according to topographic context: valley depth for low stations and magnitude of relief prominence for high stations). *Diagrammes de dispersion. Valeurs observées par rapport aux valeurs estimées pour la fréquence (tn + tx), l'intensité (tn + tx) et la durée des inversions. Les estimations sont effectuées par régression multiple où la variable expliquée est tour à tour la fréquence, l'intensité et la durée des inversions et les variables explicatives sont les cinq descripteurs topographiques décrits dans la section 3 (altitude des stations basses, altitude des stations hautes, amplitude altitudinale entre les deux stations qui composent chaque site et contexte topographique : profondeur des vallées pour les stations-basses et ampleur de l'émergence des reliefs pour les stations-hautes).*

The other descriptors are less well estimated, although the results remain significant at thresholds between 2% (Intens-tx) and 6% (duration). The minimum R^2 is 0.61 (duration), the other three are around 0.7. The RMSE of frequency and intensity inversion for tn and tx is around 10% and 0.4°C respectively.

	Frq-tn	Frq-tx	Intens-tn	Intens-tx	Duration
R^2	0.81	0.67	0.69	0.72	0.61
RMSE	9.8	10.4	0.43	0.38	0.4
p-value	0.002	0.042	0.022	0.014	0.056

Table 4: Quality measurements (R^2, RMSE and p-value) of the five estimated descriptors: frequency of inversions during tn (Frq-tn) and tx (Frq-tx), intensity of inversions during tn (Intens-tn) and tx (Intens-tx), and duration of inversions. *Mesures de la qualité (R^2, RMSE et p-value) des cinq descripteurs estimés : fréquence des inversions lors des tn (Frq-tn) et des tx (Frq-tx), intensité des inversions lors des tn (Intens-tn) et des tx (Intens-tx) et durée des inversions.*

5. Discussion

5.1. Influence of elevation

The elevation of the low stations mainly affects the characters (frequency and intensity) of the tn inversions. The fact that the Rs (frequency, intensity, and duration) for low stations are positive means that it is mainly the high-valleys, or mountain valleys, that are the most prone to inversions. This influence of elevation is less simple for high stations: the Rs are of the opposite sign between frequency ($r < 0$) and intensity ($r > 0$) of inversions. Inversions are infrequent but intense in the mountains compared to the plain if we consider the high stations. The coherence between these two points is not obvious and the process(es) responsible for these thermal behaviors is (are) not easy to identify. Despite an intense search of the literature, very little work has been found on this issue. A hypothesis can be put forward that invokes the role of wind on the weakening and/or rarefaction of inversions (Dorninger *et al*., 2011; Zardi and Whiteman, 2013). Because wind speed is higher at high elevations and in exposed sites (ridges) than over plains and in sheltered areas (topographic hollows, valley bottoms), it affects the low stations less than the high stations. Indeed, because they are located at the bottom of valleys, the low stations, whether located in the plain or in the mountains, are relatively sheltered from the wind effects that destroy inversions. If the frequency trend of tn and tx inversions as a function of the elevation of the low stations is positive, it is therefore for other reasons: perhaps because colder temperatures in the mountains promote the accumulation of stable air at the bottom of the lows. The reverse trend in the frequency of tn and tx inversions as a function of elevation at high stations is explained by the action of the wind (Hu *et al*., 2013; Van Hooijdonk *et al*., 2017), which is more turbulent in the mountains. As a result, the lower of the high stations are relatively immune to the effects of the wind, unlike the stations at higher elevation: the tendency of inversions to occur with the elevation of the upper stations is therefore negative.

The maximum frequency thus characterizes sites where the low stations are located at high elevations and where the high stations are not located too high in elevation. Site H-H1 (883 m - 981 m) is such a case, unlike sites G-G1 (801 m - 1235 m) or E-E1 (1047 m - 1228 m) where the elevation of the high station is too high. Conversely, low inversion frequencies are found at sites where the low station is located at low elevation but the high station is located at high elevation. These are regional sites but also some local sites (D-D4, 542 m - 1103 m) in particular. All these mechanisms can be contemplated but are difficult to test on the basis of statistics. To test these hypotheses, the observations would benefit from being cross-referenced with numerical modeling exercises. But neither can it be ruled out that this relationship is

dependent on station sampling. A study is being conducted throughout France that should provide some answers.

5.2. Influence of the altitudinal amplitude

The negative relationship between inversion frequency and amplitude is strong for both tn and tx (R = -0.83 and -0.60 significant at the 1% and 5% levels). This result is partly due to the influence of the four regional sites, which combine low inversion frequency and high altitudinal difference between the low and high stations. However, the correlation calculation applied only to local sites does provide lower correlation values (-0.55 and -0.43 for tn and tx significant at 5% level), but the sign is negative too. There is therefore a marked trend: the greater the altitudinal difference between the two stations of a site, the more the inversion frequency decreases. This result contrasts with the result modeled by Wagner *et al*. (2015), who concluded that "*the deeper the valley, the stronger the upvalley winds and the more favoured the formation of vertically stacked circulation cells and an elevated valley inversion layer*". To explain our result, let us take a theoretical example with a temperature set at -5 °C at the bottom of the valley where station C1 is located (figure 6). The temperature rises until the 650 m level where it reaches its maximum (-3 °C), marking the upper limit of the boundary layer. Station C2 below this limit records an inversion. Above the boundary layer, the temperature decreases with elevation with an altitudinal gradient of about 0.6 °C/100 m. At 1000 m elevation, C3 with a temperature of -5 °C reaches the same value as at the valley bottom and does not record any inversion. The highest inversion frequencies are therefore observed at sites where the high station lies close to the upper level of the boundary layer. Stations located higher in elevation, in the open atmosphere, see their temperature fall in proportion to the elevation, thus decreasing the frequency of inversions.

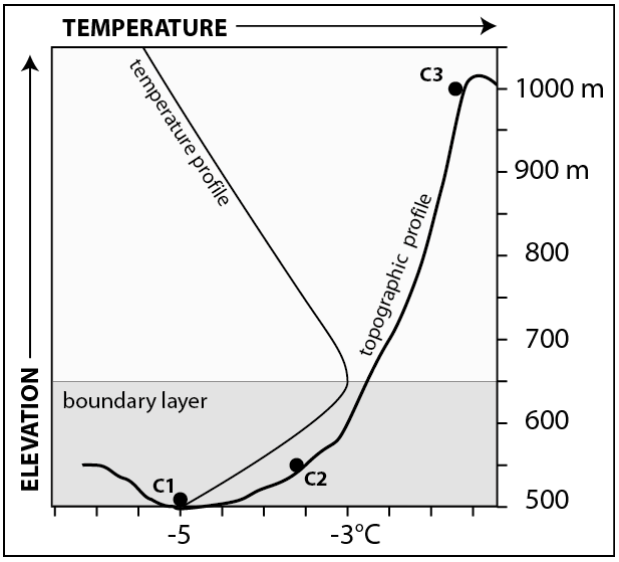

Figure 6: Theoretical diagram of the influence of altitudinal amplitude on the frequency of inversions (the values are given for information only and do not concern any particular place or season). *Schéma théorique de l'influence de l'amplitude altitudinale sur la fréquence des inversions (les valeurs sont données à titre indicatif et ne concernent aucun lieu ni saison particuliers).*

5.3. Comparison of inversion characters at two neighboring sites

The three descriptors (elevation, amplitude, and topographic landforms) were chosen to explain the spatial variation of inversion characters because they are easy to calculate. Other descriptors exist that could also explain the characteristics of the inversions: for example, solar radiation (Sadoti *et al*., 2018). To show this, we will use the example of the two neighboring sites H and F located in the east of the study area at the contact between the plateau and the folded mountains of the Jura.

Station H is located at 883 m, at the bottom of a vast, almost deforested and shallow syncline valley, (98 m amplitude between H and H1) (Table 1). Station F, 15 km away, is located 350 m lower at the bottom of a very narrow valley covered with a compact forest. Both sites are characterized by an amplitude and topographical context of their analogous high station (174 m amplitude between F and F1). The frequency and intensity of inversions are only slightly higher on the anticline than in the valley during tn (73.4% versus 72.3%); and the reverse occurs during tx. The duration of the inversion sequences is longer at the bottom of the valley. The differences observed in Table 5 are therefore well related to the shape of the hollow landform in which the low station is located. The enclosed valley is in the shade for four winter months.

	Frq-tn (%)	Frq-tx (%)	Intens-tn (°C)	Intens-tx (°C	Duration (days)
H-H1	73.4	47.9	26.5	13.5	2.5
F-F1	72.3	57.2	24.2	23.6	3.7

Table 5. Average of the inversion characters over the three years of observation (frq=frequency, intens=intensity) during tn and tx; sites H-H1 (broad anticlinal) and F-F1 (incised valley). *Moyenne des caractères des inversions lors des trois années d'observation (frq=fréquence, intens=intensité) lors des tn et des tx ; sites H-H1 (large anticlinal) et F-F1 (vallée encaissée).*

As a result, cold air even stagnates in the middle of the day (Jahanbakhshasl and Roshani, 2013; Largeron and Staquet, 2016) and possibly for persistent inversion sequences lasting more than 20 days (Joly and Richard, 2019). In the syncline valley, the vast open areas favor radiation. Inversions start easily and they are intense (Vitasse *et al*., 2017). But the thinness of the boundary layer makes them vulnerable to turbulence and morning warming so that they are easily destroyed during the day by thermal convection (Conangla *et al*., 2018).

To illustrate these thermal patterns, the temperature variations during autumn 2015 and winter 2016 are presented. These clearly show the influence of the topographical context on inversions (figure 7). The Russey Valley site (vast but shallow anticline) has the most severe inversion of the period (on 30 December, the temperature difference between the bottom of the valley, sensor H, and the top of the slope that overlooks it, sensor H1, was -15°C). But the bottom of the Reverote Valley (sensor F) is much more stable, with long inversion sequences (25 September to 7 October 2015; 30 November to 8 December 2015; 10 December to 31 December 2015) or no inversions (13 October to 19 October 2015; 25 February to 29 February 2016). During the same sequences, the Russey valley oscillated between inversion during tn and absence of inversion during tx (in Figure 7, the blue curve rises above and falls below the dashed line). The only long inversion sequence over the Russey Valley was from 30 November to 21 December 2015.

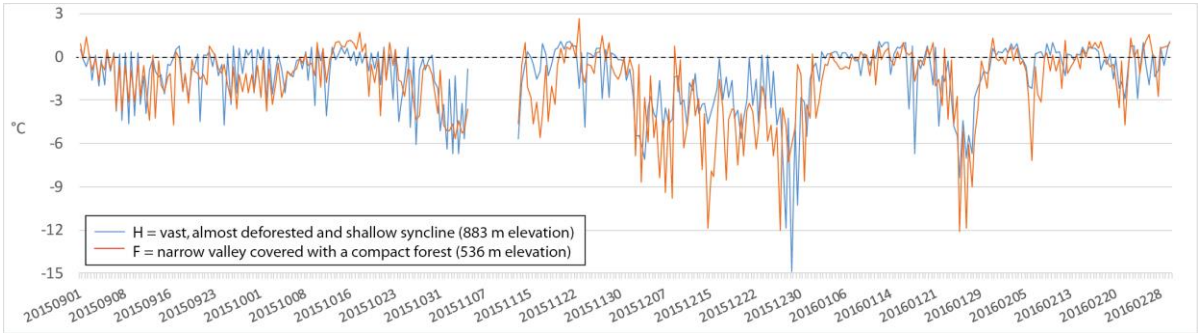

Figure 7: Temperature graph obtained from sensors (one measurement every six minutes) in January 2016 at sites H-H1 (Russey) and F-F1 (Réverotte). A negative value indicates a thermal inversion. *Graphe des températures obtenues des capteurs (une mesure toutes les six minutes) au cours du mois de janvier 2016 dans les sites H-H1 (le Russey) et F-F1 (Réverotte).*

The greater stability of temperature at the bottom of deep valleys is explained by the phenomenon of hysteresis, which had already been mentioned to explain the higher inertia of temperatures in forested sites than in open sites (Joly, 2014). It also applies here: temperature variations induced by weather changes do not result in a movement at the bottom of the deep valleys of the same magnitude as in the shallow valleys. Cold air accumulated during the inversion sequence or warm air carried to the bottom of the valley during windy advective phases tends to remain as it is after the atmospheric situation favorable to inversion or non-inversion has ceased. This decoupling from the overlying synoptic flow is more marked in deeper valleys (Daly *et al.*, 2009; Largeron and Staquet, 2016).

Conclusion

Sixteen sites distributed across the plateaus and mountains of the Jura consisting of one station at the bottom of a topographic trough and one station located at least 50 m higher are analyzed to detect which topographic factors are most relevant for explaining the spatial variations in inversion characteristics of frequency, intensity, and duration. The variations in these three characters are first explained by the descriptor "amplitude", *i.e*. the altitudinal difference between the two stations of each site. The sites that observe the most frequent inversions are those where the high station is located close to the boundary layer, around 100 m above the low station. Sites with much greater amplitudes have a lower frequency of inversions although they are more intense but shorter-lived than in the previous case.

The other two descriptors (elevation and topographical context) are good predictors, but only for one or other of the inversion characters and only in the context of tn or tx. The inversions that occur during tn are thus mainly explained by two topographical factors (elevation of the low station and valley) contrary to those that explain the inversions that occur during tx (elevation of the high station and hump). The regional climatology, frequency, and higher wind strength at elevation than in the lowlands and in the afternoons than in the mornings, was suggested as an explanation. But this hypothesis cannot readily be confirmed without additional *in situ* observations. To confirm this, for example, the demonstration should be based on a larger number of observation sites equipped with wind speed sensors.

A statistical model of the three inversion indicators was proposed via multiple regressions in which the explanatory variables are elevations of the low and high stations, altitudinal amplitude, valley (low station), and hump (high station). The results are all significant with R^2 ranging from 0.61 to 0.81. They could lead to an interpolation of the inversion indicators. We did not attempt this because the sampling of stations that does not cover all the topographical contexts of the Jura is not exhaustive. To the extent that the low stations are exclusively at the bottom of topographic troughs, the grid interpolated pixels would have been spatially aggregated into patches of varying length and width. This idea will be developed as a natural extension of this study, based not on the plateaus and mountains of the Jura but on the whole of France in order to provide more general results. It would be of the utmost interest to estimate the ability of any point of the territory to promote or, on the contrary, to hinder the establishment of inversions. Pollution by particulate matter affects urban centers primarily. But it also affects rural areas where residential wood burning is common. Knowledge of the places where inversions occur most frequently would allow developers to inform the population of the risks involved (Steward and Nitschke, 2016).

Acknowledgements: We are grateful to Météo-France for making the data available under the agreement signed with the University of Burgundy; the Zone Atelier de l'Arc

Jurassien (http://zaaj.univ-fcomte.fr); the mayors of the municipalities and private owners who allowed us to install the sensors in their forest plots.

References

Anquetin S., Guilbaud C. and Chollet J.-P., 1998. The formation and destruction of inversion layers within a deep valley. *J. Appl. Meteor*, 37, 1547-1560.

Barry R. G., 2008. *Mountain Weather and Climate*. 3rd ed. Cambridge University Press, 506 p.

Burns P. and Chemel C., 2015. Interactions between downslope flows and a developing cold-air pool. *Boundary-Layer Meteorology*, 154, 57-80.

Chemel C., Arduini G., Staquet C., Largeron Y., Legain D., Tzanos D. *et al*., 2016. Valley heat deficit as a bulk measure of wintertime particulate air pollution in the Arve River Valley. *Atmos. Env*., 128, 208-215.

Conangla L., Cuxart J., Jiménez M.A., Martínez-Villagrasa D., Ramon J., Tabarelli M.D. and Zardi D., 2018. Cold-air pool evolution in a wide Pyrenean valley. *International Journal of Climatology*, 38(6), 2852-2865, doi.org/10.1002/joc.5467.

Czarnecka M. and Nidzgorska-Lencewicz J., 2017. The impact of thermal inversion on the variability of PM10 concentration in winter seasons in Tricity. *Environment Protection Engineering*, 44(2), 157-172.

Daly C., Conklin D.R. and Unsworth M.H., 2009. Local atmospheric decoupling in complex topography alters climate change impacts. *International Journal of Climatology*, 30 (22), 1857-1864.

Dorninger M., Whiteman C.D., Bica B., Eisenbach S., Pospichal B., and Steinacker R., 2011. Meteorological events affecting cold-air pools in a small basin. *Journal Appl Meteorol Climatol*, 50, 2223-2234.

Dupont J.C., Haeffelin M., Stolaki S., Elias T., 2016. Analysis of dynamical and thermal processes driving fog and quasi-fog life cycles using the 2010–2013 ParisFog dataset. *Pure Appl. Geophys*., 173,1337-1358; doi 10.1007/s00024-015-1159-x

El Melki T., 2007. Inversions thermiques et concentrations de polluants atmosphériques dans la basse troposphère de Tunis. *Climatologie*. http://lodel.irevues.inist.fr/climatologie/index.php?id=773.

Fallot J.-M., 2012. Influence de la topographie et des accumulations d'air froid sur les températures moyennes mensuelles et annuelles en Suisse. In Bigot S. and Rome S. (eds.). 25ème colloque de l'Association Internationale de Climatologie (AIC), 273-278.

Fernando H.J.S., Verhoef B., Di Sabatino S., Leo L.S., and Park S., 2013. The Phoenix Evening Transition Flow Experiment (TRANSFLEX). *Boundary-Layer Meteorology*, 147, 443-468. doi:10.1007/s10546-012-9795-5.

Helmis C.G. and Papadopoulos K.H., 1996. Some aspects of the variation with time of katabatic flows over a simple slope. *Quarterly Journal of the Royal Meteorological Society*, 122, 595-610. doi : 10.1002/qj.49712253103.

Hu X.M., Klein P.M., Xue M., Shapiro A., and Nallapareddy A., 2013. Enhanced vertical mixing associated with a nocturnal cold front passage and its impact on near-surface temperature and ozone concentration. *Journal of Geophysical Research: Atmospheres*, 118(7), 2714-28.

Jahanbakhshasl S. and Roshani R., 2013. The study of condition and the intensity of lower level temperature inversion in Tabriz of 2004–2008. *Geographical Research*, 28(4), 45-54. doi: 10.5194/isprsarchives-XL-1-W5-357-2015.

Joly D., Brossard T., Cardot H., Cavailhès J., Hilal M., and Wavresky P., 2010. Les types de climats en France, une construction spatiale (Types of climate in continental France, a spatial construction). *Cybergeo: European Journal of Geography*, 501. http://cybergeo.revues.org/index23155.html

Joly D., Bois B., and Zaksek K., 2012. Rank-ordering of topographic variables correlated with temperature. *Atmospheric and Climate Science*, 2(2), 139-147. doi: 10.4236/acs.2012.22015.

Joly D., 2014. Etude comparative de la température en forêt et en espace ouvert dans le Parc Naturel Régional du Haut-Jura. *Climatologie*, 11. http://lodel.irevues.inist.fr/climatologie/index.php?id=562

Joly D., Gillet F., 2017. Interpolation of temperatures under forest cover on a regional scale in the French Jura Mountains. *International Journal of Climatology*, 37(S1), 659-670, DOI:10.1002/joc.5029

Joly D. and Richard Y., 2019. Frequency, intensity and duration of thermic inversions in the Jura, France. *Theor Appl Climatol*. doi.org/10.1007/s00704-019-02855-3

Kollas C., Randin C.F., Vitasse Y., and Körner C., 2013. How accurately can minimum temperatures at the cold limits of tree species be extrapolated from weather station data? *Agricultural and Forest Meteorology*, 184, 257-266.

Largeron Y. and Staquet C., 2016. Persistent inversion dynamics and wintertime PM10 air pollution in Alpine valleys. *Atmospheric Environment*, 135, 92-108. doi.org/10.1016/j.atmosenv.2016.03.045

Lundquist J.D., Pepin N., and Rochford C., 2008. Automated algorithm for mapping regions of cold-air pooling in complexterrain. *Journal Geophysical Res*earch, 113, D22107.

Mahrt, L., Richardson S., Seaman, N., and Stauffer, D., 2010. Non-stationary drainage flows and motions in the cold pool. *Tellus*, 62, 698-705. doi.org/10.1111/j.1600-0870.2010.00473.x

Mernild S.H., Liston G.E., 2010. The influence of air temperature inversions on snowmelt and glacier mass balance simulations, Ammassalik Island, Southeast Greenland. *Journal Appl Meteorol Climatol*, 49(1), 47-67. doi.org/10.1175/2009JAMC2065.1

Mirocha J.D., Branko K., 2010. Large-eddy simulation study of the influence of subsidence on the stably stratified atmospheric boundary layer. *Boundary-Layer Meteorol*, 134(1), 1-21. doi 10.1007/s10546-594 009-9449-4

Papadopoulos K.H. and Helmis C.G., 1999. Evening and morning transition of katabatic flows. *Boundary-Layer Meteor*ology, 92, 195-227. doi.org/10.1023/A:1002070526425

Pomeroy J. W. and E. Brun, 2001: Physical properties of snow. *Snow Ecology: An Interdisciplinary Examination of Snow-Covered Ecosystems*, H. G. Jones et al., Eds., Cambridge University Press, 45–126

Sadoti G., McAfee S.A., Roland C.A. Fleur N.E., Sousanes P.J., 2018. Modelling high-latitude summer temperature patterns using physiographic variables. *International Journal of Climatology*, 38(10), 4033-4042. doi: 10.1002/joc.5538

Stewart S.B. and Nitschke C.R., 2016. Improving temperature interpolation using MODIS LST and local topography: A comparison of methods in south east Australia. *International Journal of Climatology*, 37, 7, 3098-3110.

Van Hooijdonk I.G.S., Clercx H.J.H., Abraham C., Holdsworth A.M., Monahan A.H., Vignon E., Moene A.F., Baas P., and Van De Wiel, B.J.H., 2017. Near-surface temperature inversion

growth rate during the onset of the stable boundary layer. *Journal of the Atmospheric Sciences*, 74(10), 3433-49.

Vitasse Y., Klein G., Kirchner J.W., and Rebetez M., 2017. Intensity, frequency and spatial configuration of winter temperature inversions in the closed La Brevine valley, Switzerland. *Theoretical and Applied Climatology*, 130 (3-4), 1073-1083.

Wagner J.S., Gohm A., and Rotac, M.W., 2015. The impact of valley geometry on daytime thermally driven flows and vertical transport processes. *Quarterly Journal of the Royal Meteorological Society*, 141(690), 1780-94.

Williams R. and Thorp, T., 2015. Characteristics of springtime nocturnal temperature inversions in a high latitude environment. *Weather*, 70, suppl.1, S37-43, doi.org/10.1002/wea.2554.

Young M.V., 2016. Rapid temperature and wind fluctuations at a mountain site in northern England on 9/10 February 2015. *Weather*, 71(2), 32-35.

Yu L., Zhong S., Bian, X., 2017. Multi-day valley cold-air pools in the western United States as derived from NARR. *International Journal of Climatology*, 37(5), 2466-2476.

Zardi D. and Whiteman C.D., 2013. "Diurnal Mountain Wind Systems". In: Chow F., De Wekker S., Snyder B. (eds) *Mountain Weather Research and Forecasting.* Springer Atmospheric Sciences. Springer, Dordrecht, 35-119.